


# Configuration design method of hybrid electric agricultural machinery system based on layered two-dimensional matrix

Baogang LI<sup>1,2\*</sup>, Jinbo PAN<sup>1</sup> , Rui SUN<sup>1</sup>, Yuhuan LI<sup>1</sup>, Zunmin LIU<sup>1</sup>, Wanyou HUANG<sup>2</sup>, Hanjun JIANG<sup>1</sup>, and Fuhao LIU<sup>1</sup>

<sup>1</sup>School of Mechanical and Automotive Engineering, Qingdao University of Technology, Qingdao 266520, China

<sup>2</sup>Key Laboratory of Transportation Industry for Transport Vehicle Detection, Diagnosis and Maintenance Technology, Jinan 250357, China

**Abstract.** The working environment and objects of agricultural machinery are different from those of automobiles, and agricultural machinery is greatly affected by such working environment and working conditions, while its power output system is more complex. Agricultural machinery not only has drive output, but also PTO output and hydraulic output, which together constitute the output system of agricultural machinery. Agricultural machinery conditions can be divided into road transportation working conditions and field operation working conditions. The working conditions of agricultural machinery can be divided into different load conditions according to the different traction tools and whether the hydraulic and PTO work, such as ploughing, rotary tillage, fertilization and transportation. Therefore, developing hybrid electric agricultural machinery systems that are suitable for various complex working conditions holds great theoretical significance and practical value. This should be done bearing mind the complex working conditions of agricultural machinery systems in agricultural work and the intricate challenges in designing hybrid agricultural machinery systems. In this paper, a two-dimensional matrix is used to represent the physical structure and dynamics of the multi-channel power output agricultural mechanism. A hierarchical two-dimensional matrix method for the generation and screening of hybrid electric agricultural machinery systems with multi-power output power is also proposed. The components of agricultural machinery are divided into an input layer and an output layer, and these components are coded and defined, and then transformed into a matrix. The hierarchical two-dimensional matrix method is used to generate and screen the hybrid electric agricultural mechanism type. Through the stratification of the matrix, complexity of the configuration generation is reduced, and the constraints are applied to the basic screening of the configurations generated. The rationality of the configurations obtained after generation and screening is verified by Simulink simulation. The results show that the configuration screened by this method can meet the performance requirements of agricultural machinery.

**Keywords:** composite power; agricultural machinery; multi-power output; two-dimensional matrix.

## 1. INTRODUCTION

As an important field widely used by high technology, agriculture has been changed by the progress of engineering knowledge as early as the last century [1]. With the aging of China's population, more and more rural population migrate to cities and towns. This leads to a decline in agricultural productivity [2]. Agriculture has changed because of the technological innovation of agricultural machinery. Its productivity has not only been greatly improved but also the risk of operating agricultural machinery has been reduced [3]. However, traditional tractors are not conducive to resource utilization and environmental protection due to their high fuel consumption and high emissions [4]. The agricultural tractor experiences complex working conditions, many working modes and a large speed ratio range [5]. With the development of modern agriculture, agricultural machinery is also moving towards diversified and intelligent technologies. And currently research on agricultural machinery is gradually moving towards

new energy. It has been found that batteries, fuel cells (FC), supercapacitors (SC) and solar energy can be used as power sources for hybrid systems [6]. Electric drives for agricultural machinery such as tractors can reduce fuel consumption, reduce noise, and be more conducive to controlling torque and speed, thereby improving work quality [7]. At present, hybrid power systems can save fossil fuels and reduce pollution, to solve the problems of environment and traffic [8]. Therefore, the combination of a hybrid power system and traditional agricultural machinery will solve the problems of energy loss and environmental pollution. Based on AD and extenics, combined with the advantages of electric tractors and traditional tractors, Li *et al.* [9] proposed a new type of tractor power transmission system structure that can enable the entire machine to adapt to various complex working conditions. However, at present, only the already existing hybrid power system is applied to the agricultural machinery system, which cannot fully solve the issue of complex working conditions of the agricultural machinery system. Compared with automobiles, agricultural machinery systems meet more complex working conditions and have more input and output components. Therefore, it is necessary to propose a method for generating, screening and optimizing agricultural machinery types based on hybrid power systems.

\*e-mail: [baog\\_li@alu.cqu.edu.cn](mailto:baog_li@alu.cqu.edu.cn)

Manuscript submitted 2024-05-10, revised 2024-07-01, initially accepted for publication 2024-07-22, published in November 2024.

At present, the hybrid power system can be divided into three types: series configuration, parallel configuration and hybrid configuration.

Jia *et al.* [10] established a HEAT tractor model with high dynamics and energy fidelity for tandem HEAV tractors. Francesco *et al.* [11–13] designed and optimized the energy management of the parallel hybrid tractor, and then compared it with the series configuration. Finally, it is found that the parallel configuration performs well in peak power performance, while the series configuration has the highest fuel saving rate. Claudio *et al.* [14] designed a fully hybrid power transmission system based on electric stepless transmission (e-CVT). Its performance is similar to that of traditional tractors, but it has the function of a hybrid power system.

The motor size of the hybrid configuration is smaller than that of the series configuration, and the engine size of the hybrid configuration is smaller than that of the parallel configuration [15]. Among them, the planetary row is an important part of the hybrid system. Planetary gear is usually used to distribute the power of the engine to the wheels and generators, while also achieving power deceleration or growth, such as in the Toyota Prius hybrid system [16–18]. Through the planetary gear train, the series-parallel hybrid system can achieve efficient energy conversion and distribution in different operating modes, because the agricultural machinery system has multiple outputs, and the structure is relatively more complex. Therefore, a design method is needed now, and a variety of novel hybrid agricultural machinery systems are designed by this method.

At present, there are three main screening methods for hybrid power systems: leverage method [19], “D” matrix [20], and the graph theory method [21].

The above three methods simplify the complex system into a simple topology by analyzing the structure and characteristics of the system and then generating the whole configuration. They are of great significance for the later research and development of hybrid power systems. However, the above methods are proposed for hybrid electric vehicle configurations. For multi-output configurations such as agricultural machinery, there is no systematic configuration generation scheme.

Therefore, this paper aims to explore the configuration generation method of multi-channel power output based on a hybrid power system by the hierarchical multi-dimensional matrix method.

## 2. LAYERED TWO-DIMENSIONAL MATRIX METHOD

### 2.1. Construction of layered two-dimensional matrix

The hybrid system is mainly composed of the engine (E), motor (MG), gearbox (A), planetary gear and power output components (V). The engine, motor and gearbox are defined as the input layer components, while the drive output, PTO output and hydraulic output are defined as the output layer components. As the power input system, the engine (E), motor (MG) and other components are connected with the power output components (V) through the planetary row, to achieve the purpose of arbitrarily switching various modes. As shown in Figs. 1 and 2, the

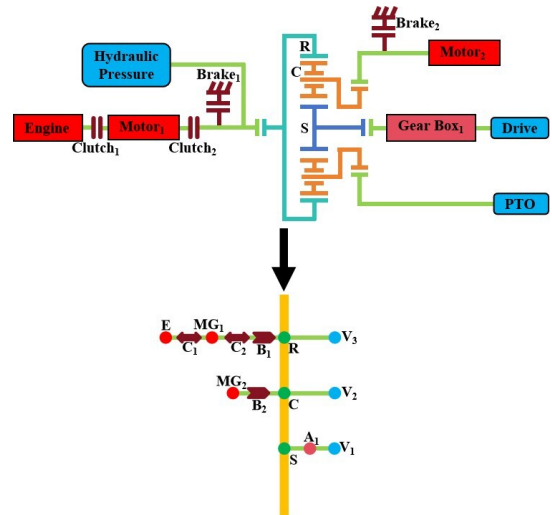


Fig. 1. Representative topological configuration of the single-planetary row

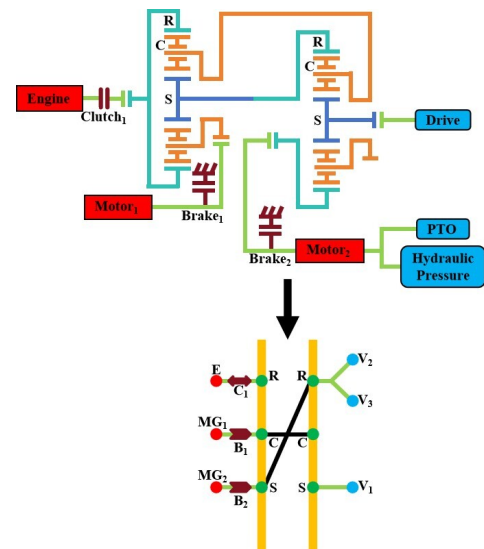


Fig. 2. Representative topological configuration of the dual row

multi-power output hybrid electric agricultural mechanism can be simplified into a simple topological structure diagram. As shown in Table 1, every single component is represented by an individual part of the topology graph.

Table 1

Meaning of each part in topological graph

| Symbol    | Representation of components |
|-----------|------------------------------|
| ● (Red)   | Input components             |
| ● (Blue)  | Output components            |
| ● (Green) | Planetary row components     |
| ● (Pink)  | Gear box                     |
| ➔ (Red)   | Brake                        |
| ↔ (Red)   | Clutch                       |

Configuration design method of hybrid electric agricultural machinery system based on layered two-dimensional matrix

According to the coding of the components in Table 2, the configuration in Fig. 1 can be equivalent to a matrix, that is:

$$\begin{bmatrix} 1 & 2 & 4 & 0 & 9 \\ 0 & 2 & 5 & 0 & 8 \\ 0 & 0 & 6 & 3 & 7 \end{bmatrix}$$

the engine and motor are defined as input components, i.e. components for adjusting torque and the speed ratio. Drive output, PTO output and hydraulic output are defined as output components.

**Table 2**  
Coding of each component

| Component    | Coding | Component           | Coding | Component                            | Coding |
|--------------|--------|---------------------|--------|--------------------------------------|--------|
| Engine (E)   | 1      | Ring gear (R)       | 4      | Drive (V <sub>1</sub> )              | 7      |
| Motor (MG)   | 2      | Planetary shelf (C) | 5      | PTO (V <sub>2</sub> )                | 8      |
| Gear box (A) | 3      | Sun gear (S)        | 6      | Hydraulic pressure (V <sub>3</sub> ) | 9      |

According to the above simplified topological configuration diagram and its corresponding matrix, the left side of the planetary row is composed of input components, and the right side of the planetary row is composed of output components. Therefore, the matrix can be divided into two layers, namely, the input layer matrix and the output layer matrix. Therefore, only the input layer matrix and the output layer matrix need to be determined. The combination of the two is a large matrix, which is a multi-power output hybrid electric configuration based on the planetary row.

According to the coding of each component in Table 1 and the above definition, the input layer is composed of two components, which are engine and motor, and the corresponding elements are 1 and 2, respectively. The input layer matrix is defined as a 3 × 3 matrix, and element 0 is added to the input layer. The 0 element indicates that the node has no component connection.

The above three elements are combined, and then the combined vectors are randomly arranged and combined. Ultimately, the final input layer matrix can be obtained by evaluating and selecting constraint condition I in Table 3. The specific generation and screening process is shown in Fig. 3.

**Table 3**  
Constraint condition I

|   |  |
|---|--|
| 1 | Calculate the sum H of all elements in the matrix;<br>3 ≤ H ≤ 13 |
| 2 | Determine whether the matrix contains vector 1 and vector 2      |
| 3 | Determine whether the same row in the matrix has the same vector |

The above diagram can be divided into four steps:

**Step 1:** Through the random combination of coding, a total of 125 matrices are generated;

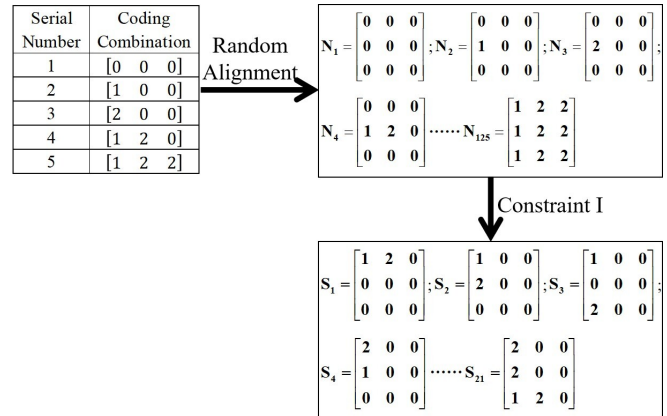


**Fig. 3.** Single-planetary row input layer matrix generation screening

**Step 2:** Summing up all the matrices to obtain the sum of the numbers of each matrix H. According to the range of H in Table 2, the matrix that does not meet the conditions is initially deleted;

**Step 3:** The vector discrimination of the residual matrix is carried out. Because the configuration must contain the engine and the motor, the presence or absence of code 1 and code 2 is used as the basis for secondary screening; delete the matrix that does not contain code 1 and code 2. Keep the matrix containing code 1 and code 2.

**Step 4:** Again, the same discrimination is performed on the vectors in the residual matrix. Since the same components in the configuration cannot be connected, it is judged whether each row in the matrix has the same vector. If a row in the matrix has the same vector, it is determined that the matrix does not meet the constraints.

In summary, after the above four steps of screening, a total of 21 input layer matrices can be obtained.

The output layer is composed of three parts: drive output, PTO output and hydraulic output. The above three output forms can be divided into three independent output forms, two outputs in parallel with another independent output form, and three outputs in parallel.

It can be seen from Table 1 that the above three output elements are 7, 8 and 9, respectively. Therefore, the generation and screening process of the output layer is similar to the input layer process, and both are in the form of a 3 × 3 matrix. Similarly, the element 0 should be added to combine the four elements. The combined vectors are randomly arranged and combined three times in a row. Finally, the output layer matrix that satisfies the conditions can be obtained by applying constraint condition II in Table 4.

After screening, a total of 27 eligible matrices are obtained.

Therefore, the combination of the input layer matrix and the output layer matrix forms a multi-power output single-planetary

**Table 4**  
Constraint condition II

|   |   |
|---|---|
| 1 | The output layer must contain three outputs               |
| 2 | None of the outputs in the output layer can be duplicated |

configuration because the engine cannot be directly connected to the drive output. And when the engine and the motor are connected to two different nodes of the planetary row and are not connected to other input and output components, the engine can be connected to the motor. In addition, we define that when the gearbox in the topology is connected to the left side of the planetary row, then the gearbox is connected in front of the planetary row in the configuration. When the gearbox in the topology diagram is connected to the right side of the planetary row, it means that the gearbox is connected to the rear of the planetary row in the configuration. Therefore, there are 6 connection modes between a single gearbox and a planetary row, and 15 connection modes between two gearboxes and a planetary row.

In summary, after re-screening the above conditions, a total of 17,820 single-planetary row configurations were generated. The representative configuration is shown in Fig. 4, and the number of individual configurations is shown in Fig. 5.

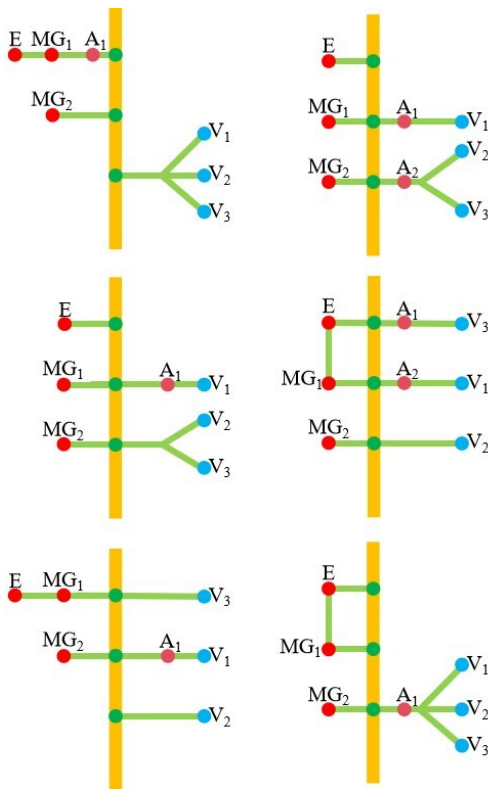


Fig. 4. Single planetary row representative configurations generated

Total number of single planetary configurations

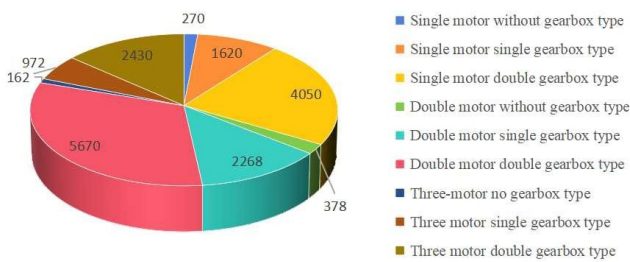


Fig. 5. Number of single-planetary row configurations

## 2.2. Generation of double planetary row configuration

A similar method can be used to screen the configuration of the double planetary row. Since the dual planetary row is connected by two single planetary rows, it can be combined into a four-node planetary row and a five-node planetary row, as shown in Fig. 6.

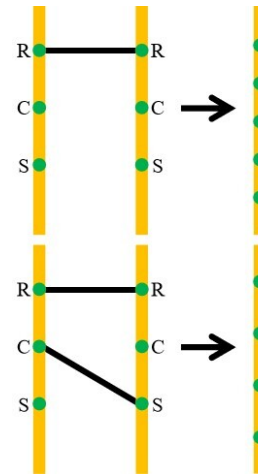


Fig. 6. Double planetary row structure

Therefore, the generation and screening of double planetary row configurations can be divided into two parts: four-node planetary row and five-node planetary row. Among them, the four-node planetary row needs to be constructed as a  $4 \times 3$  matrix. Similarly, the four elements are arranged and combined, and the four-node input layer is obtained through the screening of constraints. The process of screening is shown in Fig. 7.

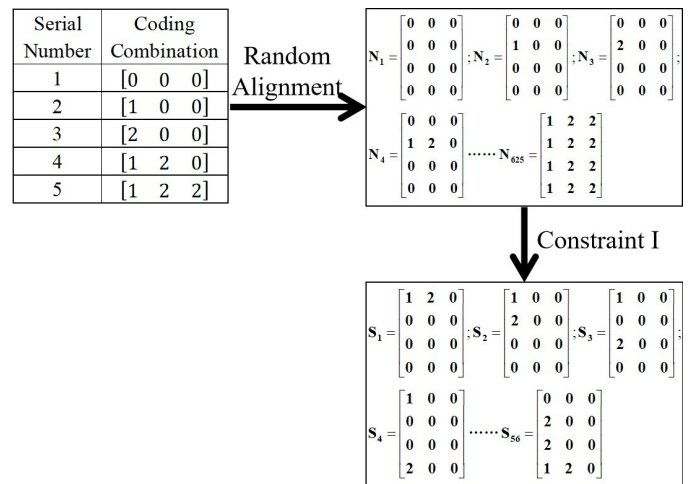


Fig. 7. Four-node double planetary row input layer matrix generation screening process

The screening principle of the input layer matrix of the double planetary row is the same as that of the single planetary row. Therefore, the screening steps of the input layer matrix of the double planetary row are basically the same as those of the single planetary row.



Because of the need to generate a  $4 \times 3$  matrix, the five coding combinations in the figure need to be randomly arranged and combined four times. Therefore, a total of 625 matrices are generated. By applying constraint I to all the above matrices, 56 input layer matrices can be obtained.

The generation and screening process of the four-node double planetary row output layer matrix is basically the same as that of the single planetary row output layer. And the screening conditions are constraint condition II in Table 4. Therefore, by repeating the generation and screening process of the output layer of a single planetary row, 64 output layer matrices can be obtained.

The configuration generation condition of the four-node double planetary row is the same as that of the single planetary row, and the double planetary row does not add the gearbox.

Therefore, there are 6,720 types of four-node two-planetary-row multi-power output single-planetary-row configurations, which are represented in Fig. 8.

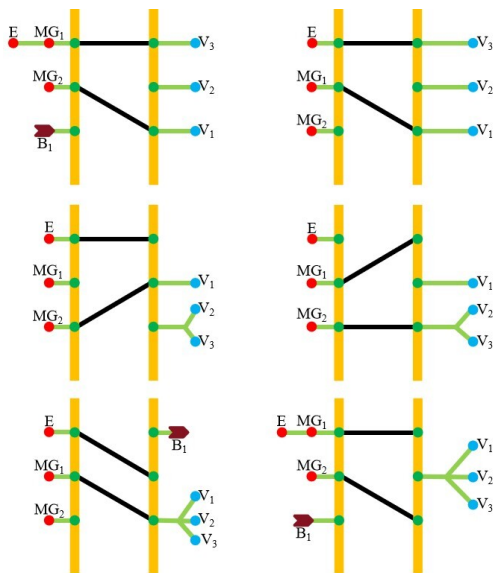


Fig. 8. Four-node double planetary row representative configurations generated

The process of the five-node planetary row is similar to that of the four-planetary row method, so it is not further explained herein. Repeating the above steps, a total of 28,520 types of five-node double-planetary-row multi-power output hybrid electric agricultural machinery systems can be obtained.

Therefore, there are a total of 35,240 types of double planetary row multi-power output hybrid electric agricultural machinery systems, and the number of configurations is shown in Fig. 9.

In summary, there are 17,820 single-planetary and 35,240 double-planetary configurations.

Brakes and clutches play an important role in the configuration. Li *et al.* [22] designed a new power shift transmission. It can achieve high transmission efficiency, reasonable gear allocation and high fuel economy of agricultural machinery. Dual-mode and multi-mode configurations usually require mode-switching components to switch modes, so the number of configurations

Total number of double planetary row configurations



Fig. 9. Number of double-planetary row configurations

can be increased by increasing or decreasing the number of brakes and clutches and changing their positions. The main function of the brake is to slow down the moving vehicle until it stops. The brake converts the motion energy of the vehicle into heat energy by generating friction, thereby achieving the effect of deceleration or parking. The main function of the clutch is to ensure the smooth start of the car and to achieve a smooth shift. During the driving process of the car, the driver can press down or loosen the clutch pedal as needed, so that the engine and the gearbox are temporarily separated and gradually engaged to cut off or transmit the power input from the engine to the transmission. In short, the brake is responsible for deceleration and parking, while the clutch is responsible for smooth starting and shifting, and it protects the transmission system from overload damage. The collaborative work of these two components enables the vehicle to drive safely and smoothly.

Therefore, the clutch and brake are also added to the generated configuration by means of a matrix. As shown in Table 5, this is a coded combination representation of the two components of the configuration. The clutch and brake are represented by C and B, respectively. The connection position of the brake is such that one end is fixed on the frame and the other end is fixed on the planetary row moving member to be braked. The clutch can be fixed between the planetary row node and the node or between the two components.

Table 5

Coding combination of two components

|       |       |       |
|-------|-------|-------|
| [1 0] | [7 0] | [7 8] |
| [2 0] | [8 0] | [7 9] |
| [1 2] | [9 0] | [8 9] |

Brake B and clutch C can be represented by vectors in Table 6.

Table 6

Coding combination of two components

|         |         |         |         |
|---------|---------|---------|---------|
| [1 B 0] | [1 C 0] | [2 C 0] | [7 C 8] |
| [1 2 B] | [1 C 2] | [8 C 0] | [7 C 9] |
| [2 B 0] | [1 2 C] | [9 C 0] | [8 C 9] |

By adding the layout of the above brake and the layout of the clutch to the configuration generated, the single planetary row multi-mode configuration and the double planetary row multi-mode configuration can be obtained, as shown in Figs. 10 and 11.

B. Li, J. Pan, R. Sun, Y. Li, Z. Liu, W. Huang, H. Jiang, and F. Liu

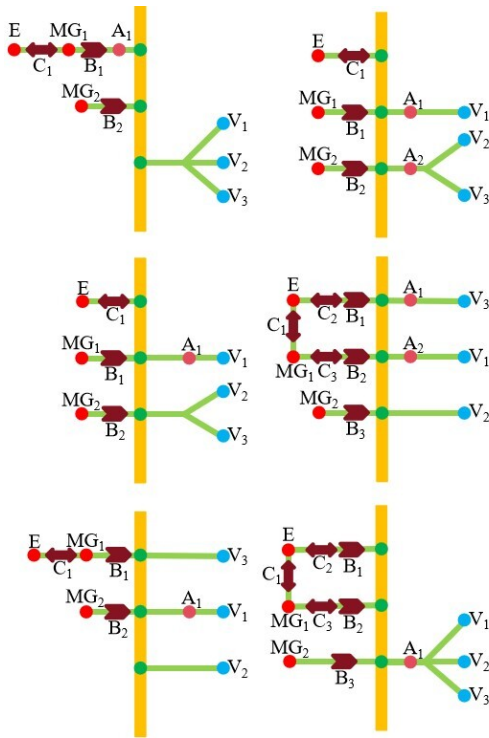


Fig. 10. Multi-mode configurations of single-planetary row

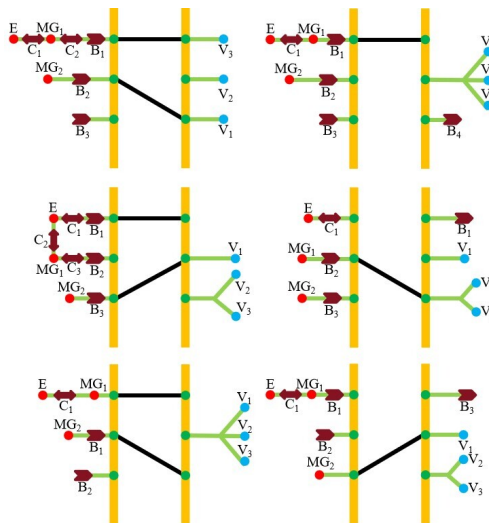


Fig. 11. Double planetary row multi-mode configurations

### 3. MODELING AND SIMULATION OF CONFIGURATION

Through the analysis of the planetary row, the relationship between the speed and torque of each node of the planetary row can be obtained:

$$T_S : T_R : T_C = 1 : k : -(1+k), \quad (1)$$

$$\omega_S + k\omega_R - (1+k)\omega_C = 0. \quad (2)$$

In the formula,  $T_S$ ,  $T_R$  and  $T_C$  are the torques of the sun gear, ring gear and planet carrier, respectively.  $\omega_S$ ,  $\omega_R$  and  $\omega_C$  are the rotational speed of the sun gear, ring gear and planet carrier, respectively.  $k$  is the characteristic parameter of the planetary

row, i.e. the ratio of the number of teeth of the ring gear to the number of teeth of the sun gear.

Hybrid electric agricultural machinery experiences traction mainly through the traction of agricultural machinery for field operations or traction for transportation operations. Therefore, the traction balance equation of agricultural machinery under traction operation conditions is:

$$F_T = F_P + F_f. \quad (3)$$

Among them,  $F_T$  is the driving force,  $F_P$  is the traction resistance, and  $F_f$  is the driving resistance.

Traction force is an important part of the resistance of agricultural machinery in the process of farming. It has a great influence on the running state of the tractor [23]. When the agricultural machinery is ploughing, the traction resistance formula is:

$$F_P = z \times b \times h \times k_p. \quad (4)$$

Of which:  $z$  is the number of ploughshares;  $b$  is the width of a single ploughshare;  $h$  is the tillage depth; and  $k_p$  is the soil specific resistance.

When the agricultural machinery undergoes the driving process, the driving wheel resistance formula is:

$$F_f = mgf \cos \theta + mg \sin \theta. \quad (5)$$

In the formula,  $F_f$  is the vehicle traction force;  $m$  is the quality of the whole machine;  $g$  is the acceleration of gravity;  $f$  is the rolling resistance coefficient;  $\theta$  is the slope.

The rotation dynamic equation of the driving wheel is:

$$J \frac{d\omega_w}{dy} = T_D - F_x r - T_f. \quad (6)$$

In the formula,  $J$  is the rotational inertia of the driving wheel;  $\omega_w$  is the rotation angular velocity of the driving wheel;  $T_D$  is the driving torque of the driving wheel;  $F_x$  is the longitudinal force of the wheel;  $r$  is the radius of the driving wheel;  $T_f$  is the rolling resistance moment.

The formula of agricultural machinery traction power is:

$$P_T = \frac{F_T \times v}{3600}. \quad (7)$$

Agricultural tractors are usually equipped with diesel engines, so the steady-state model of the engine is established based on the experimental data modeling method, and the formula can be written as:

$$B_e = f(\omega_e, T_e). \quad (8)$$

where,  $B_e$  is the fuel consumption rate;  $\omega_e$  is the engine input speed (rpm); and  $T_e$  is the engine input torque (N·m).

The motor power can be obtained by the following formula:

$$P_m = \omega_m * T_m / \eta_m. \quad (9)$$

The motor efficiency formula is:

$$\eta = \eta(\omega_m, T_m). \quad (10)$$

When the motor is running, the demand current calculation formula is:

$$I = \frac{T_m \cdot \omega_m}{9549 \cdot U_m \cdot \eta_m} \tag{11}$$

In the formula,  $\omega_m$  is the motor speed;  $T_m$  is the motor torque;  $\eta_m$  is the motor efficiency;  $P_m$  is the motor power;  $I$  is the motor demand current; and  $U_m$  is the motor load voltage.

The battery model uses a simplified power-internal resistance model. According to the battery model, the following formulas can be established:

$$U = E - IR,$$

$$SOC = \frac{C - \int I dt}{C} \tag{12}$$

In the formula,  $U$  is the output voltage of the battery;  $I$  is the battery output current;  $E$  is the electromotive force of the battery;  $R$  is the internal resistance of the battery;  $C$  is the total capacity of the battery.

Some important parameters of the simulation model are shown in Table 7 below.

**Table 7**

Configuration parameters of main components of the model

|                                   |        |
|-----------------------------------|--------|
| Quality of the whole machine (kg) | 5000   |
| Windward area (m <sup>2</sup> )   | 10.05  |
| Air resistance coefficient        | 0.8    |
| Air density (kg/m <sup>3</sup> )  | 1.29   |
| Wheel radius (m)                  | 0.9559 |
| Rolling resistance coefficient    | 0.05   |
| Main reducer transmission ratio   | 6.1    |
| Maximum engine speed (r/min)      | 3600   |
| Maximum engine torque (Nm)        | 1200   |
| Maximum motor speed (r/min)       | 7000   |
| Maximum torque of motor (Nm)      | 230    |
| Battery capacity(Ah)              | 55     |

#### 4. RESULT AND DISCUSSION

In this paper, the hybrid electric agricultural mechanism type is generated by using the layered two-dimensional matrix method. According to the demand of agricultural machinery and the actual operation situation, any choice can be made. At the same time, according to the working needs of agricultural machinery, the number of clutches and brakes can be increased or reduced to select the type of agricultural machinery that meets the needs. As shown in Fig. 12, the appropriate working mode can be selected according to the number of clutches and brakes and the working state. Such as power split mode, single motor drive mode, dual motor drive mode, engine single drive mode and pure electric mode, etc. In addition, when the hybrid agricultural machinery system adopts the double planetary row configuration, the configurations available will be more abundant.

As shown in Fig. 13a, a dual planetary configuration is adopted. The ring gear is fixedly locked. It can be ensured that one motor is coupled through a planetary gear, and the other motor can be connected in parallel. This prevents the clutch from switching back and forth. And its transmission efficiency is a high, compact structure. Four clutches and three brakes are used in the configuration shown in Fig. 13b. It can achieve the purpose of switching various working modes by controlling the working state of the clutch and brake.

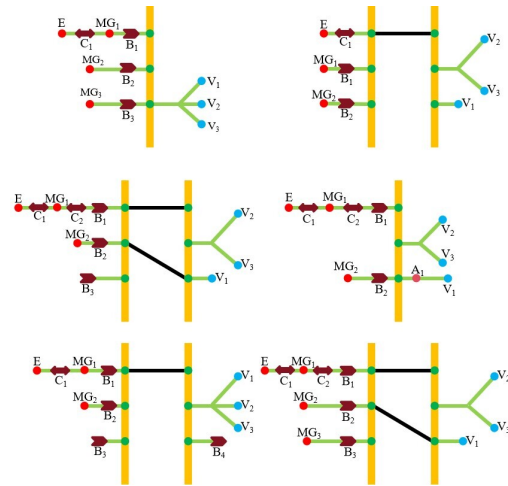


**Fig. 12.** Other multi-power output hybrid agricultural electric mechanism types

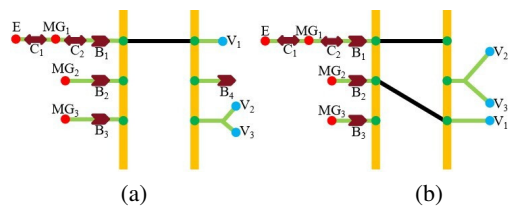


**Fig. 13.** Multi-mode configurations of double planetary row

To verify the feasibility of the configuration generated by this method, a variety of configurations are simulated and tested, and the feasibility of the method is verified by testing its dynamic performance. Firstly, the configuration is accelerated for 600 s, and the final speed that each configuration can achieve in 600 s is the maximum speed. As shown in Fig. 14, the maximum speed of the configuration is within 600 s.

According to the PowerMix test project formulated by the German Agricultural Association through international standards and regulations, the speed required for agricultural machinery is 9km/h when the load is 100% under traction work, so it can be used as a standard to evaluate the above configuration.

It can be seen from Fig. 14 that the speed of the red pentagram in the figure can reach 9 km/h. A total of 18 configurations meet the requirements. Some configurations can reach 14 km/h while keeping the throttle opening constant. However, the blue quadrilateral markers in the picture do not reach the expected speed, and some of them have a maximum speed of only 8.9 km/h, while some configurations have a maximum speed of

only 5.8 km/h. In summary, a total of 18 configurations meet the dynamic requirements. Therefore, the simulation analysis of acceleration time performance is conducted for the aforementioned configurations that achieve the anticipated maximum speed in order to evaluate the time taken to reach optimal speed. The results are shown in Fig. 15.

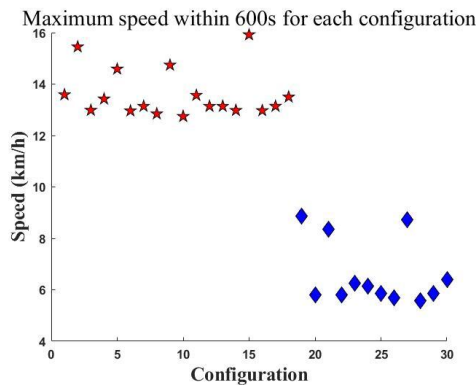


Fig. 14. Maximum velocity of configuration

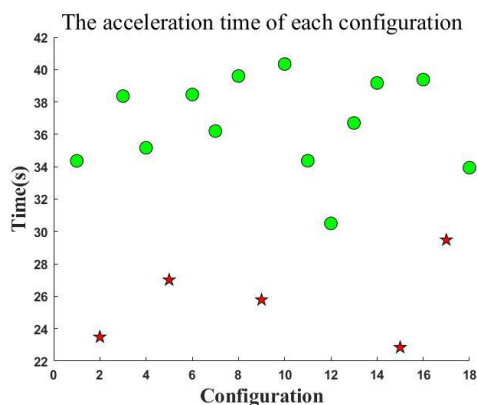


Fig. 15. Acceleration time of each configuration

From Fig. 15, it can be seen that the configurations of the red pentagram markers in the figure all reach the expected speed within 30 seconds. The fastest can reach it in 22.9 seconds. The green circle in the figure represents the remaining 13 configurations that do not reach the expected speed within 30 s, and the slowest is 40.3 s. Therefore, further control strategy simulation analysis is carried out for the above five configurations.

Therefore, this paper builds a control strategy for the above five configurations and uses the tractor cycle condition to simulate them. The above five configurations are simulated and analyzed respectively, and the resulting diagram shown in Fig. 16 can be obtained.

Through the simulation results of the above diagram, it can be found that the above five configurations can meet the cycle conditions of the vehicle, and the performance is satisfactory. Through the simulation results, it can be found that the figure shows the performance of the vehicle under each speed segment during the acceleration of the vehicle from the stationary state to maximum speed. By analyzing this diagram, we can find that the performance of the vehicle shows different characteristics in

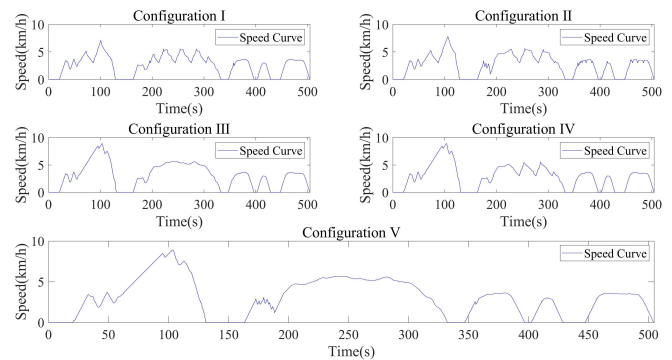


Fig. 16. Velocity following of five configurations

the three different speed ranges, i.e. low speed, medium speed and high speed.

It can be seen from the figure that the vehicle has good acceleration performance at low speed. Into the medium speed range, the performance of the vehicle is more comprehensive. In this speed range, the vehicle needs to take into account both fuel economy and power performance. The power output of the vehicle is still abundant. When the vehicle enters the high-speed range, the vehicle needs to maintain a stable driving state while providing sufficient power output. It can be seen from the figure that the performance of the vehicle at high speed is still excellent. The engine can maintain efficient operation, and the transmission can also select the optimal gear based on changes in speed and load.

In summary, according to the proposed multi-dimensional hierarchical matrix method, the filtered configuration can be generated to meet the driving needs of agricultural machinery. And the configuration generated by the hierarchical two-dimensional matrix method can be reasonably selected according to the different needs of agricultural machinery in the working process.

## 5. CONCLUSIONS

At present, the hybrid power system is becoming increasingly well-known and accepted. The configuration of hybrid electric vehicles is also being studied, and an increasing number of hybrid electric vehicles are being produced. However, there are few studies on hybrid agricultural machinery systems as compared to hybrid vehicles. The combination of a hybrid power system and a traditional tractor will be a good solution to the problem of fuel emissions caused by traditional tractors, so researching hybrid tractors is highly necessary and feasible.

In this paper, a generation and screening method based on multi-channel power output configuration is proposed by analyzing the connection relationship between the engine, motor, gearbox, output mechanism and planetary row. Through this method and Matlab function operation, different types of single-planet configurations and double-planet configurations are obtained. The one-planetary configuration generated was simulated, and the simulation results met the requirements. Some of the configurations can reach a maximum speed of 16km/h under traction load, which meets the speed requirements of the tractor working conditions. The acceleration performance was good, and the



expected speed can be reached in 22.9 seconds at the fastest. In summary, the important research is as follows:

1. Through the method of layered two-dimensional matrix, many configurations of a hybrid agricultural machinery system based on multi-power output are preliminarily screened out, and further screening will be carried out in the future.
2. The proposed design method can arbitrarily generate various configurations of planetary rows and different input and output components. Applying this method to multi-power output configurations, many configurations with excellent performance can be obtained.
3. The dynamic performance and acceleration performance of the configuration generated were simulated and tested respectively, and the configuration with better dynamic performance was selected.

## ACKNOWLEDGEMENTS

The authors would like to thank Qingdao University of Technology and Shandong Jiaotong University for the support and contribution. This work was supported by the National Natural Science Foundation of China (grant number 52202508); the Shandong Provincial Postdoctoral Foundation Project (Innovation Project) (SDCX-ZG-202400208), the Key Lab of Industrial Fluid Energy Conservation and Pollution Control, the Ministry of Education (grant number 2022-JXGCKFKT-YB-04); and the Key Laboratory of Transportation Industry for Transport Vehicle Detection, Diagnosis and Maintenance Technology (grant number JTZL2202).

## REFERENCES

- [1] G.F. Sassenrath *et al.*, "Technology, complexity and change in agricultural production systems," *Renew. Agr. Food Syst.*, vol. 23, no. 4, pp. 285–295, 2008, doi: [10.1017/s174217050700213x](https://doi.org/10.1017/s174217050700213x).
- [2] X. Gao, G. Xie, J. Li, G. Shi, Q. Lai, and Y. Huang, "Design and validation of a centrifugal variable-diameter pneumatic high-speed precision seed-metering device for maize," *Biosyst. Eng.*, vol. 227, pp. 161–181, 2023, doi: [10.1016/j.biosystemseng.2023.02.004](https://doi.org/10.1016/j.biosystemseng.2023.02.004).
- [3] E. Cavallo, E. Ferrari, L. Bollani, and M. Coccia, "Strategic management implications for the adoption of technological innovations in agricultural tractor: the role of scale factors and environmental attitude," *Technol. Anal. Strateg. Manage.*, vol. 26, no. 7, pp. 765–779, 2014, doi: [10.1080/09537325.2014.890706](https://doi.org/10.1080/09537325.2014.890706).
- [4] A. Malik and S. Kohli, "Electric tractors: Survey of challenges and opportunities in India," *Mater. Today-Proc.*, vol. 28, pp. 2318–2324, 2020, doi: [10.1016/j.matpr.2020.04.585](https://doi.org/10.1016/j.matpr.2020.04.585).
- [5] B. Li *et al.*, "Optimization Method of Speed Ratio for Power-Shift Transmission of Agricultural Tractor," *Machines*, vol. 11, no. 4, p. 438, 2023, doi: [10.3390/machines11040438](https://doi.org/10.3390/machines11040438).
- [6] M.A. Hannan, F.A. Azidin, and A. Mohamed, "Hybrid electric vehicles and their challenges: A review," *Renew. Sust. Energ. Rev.*, vol. 29, pp. 135–150, 2014, doi: [10.1016/j.rser.2013.08.097](https://doi.org/10.1016/j.rser.2013.08.097).
- [7] G.P. Moreda, M.A. Muñoz-García, and P. Barreiro, "High voltage electrification of tractor and agricultural machinery – A review," *Energy Conv. Manag.*, vol. 115, pp. 117–131, 2016, doi: [10.1016/j.enconman.2016.02.018](https://doi.org/10.1016/j.enconman.2016.02.018).
- [8] M. Ehsani, K.V. Singh, H.O. Bansal, and R.T. Mehrjardi, "State of the Art and Trends in Electric and Hybrid Electric Vehicles," *Proc. IEEE*, vol. 109, no. 6, pp. 967–984, 2021, doi: [10.1109/jproc.2021.3072788](https://doi.org/10.1109/jproc.2021.3072788).
- [9] J. Li, X. Wu, X. Zhang, Z. Song, and W. Li, "Design of distributed hybrid electric tractor based on axiomatic design and Extenics," *Adv. Eng. Inform.*, vol. 54, p. 101765, 2022, doi: [10.1016/j.aei.2022.101765](https://doi.org/10.1016/j.aei.2022.101765).
- [10] C. Jia, W. Qiao and L. Qu, "Modeling and control of hybrid electric vehicles: a case study for agricultural tractors," in *2018 IEEE Vehicle Power and Propulsion Conference (VPPC)*, IEEE, pp. 1–6, 2018, doi: [10.1109/VPPC.2018.8604997](https://doi.org/10.1109/VPPC.2018.8604997).
- [11] F. Mocera, "A Model-Based Design Approach for a Parallel Hybrid Electric Tractor Energy Management Strategy Using Hardware in the Loop Technique," *Vehicles*, vol. 3, no. 1, pp. 1–19, 2020, doi: [10.3390/vehicles3010001](https://doi.org/10.3390/vehicles3010001).
- [12] F. Mocera, V. Martini, and A. Somf, "Comparative Analysis of Hybrid Electric Architectures for Specialized Agricultural Tractors," *Energies*, vol. 15, no. 5, p. 1944, 2022, doi: [10.3390/en15051944](https://doi.org/10.3390/en15051944).
- [13] F. Mocera and A. Somf, "Analysis of a Parallel Hybrid Electric Tractor for Agricultural Applications," *Energies*, vol. 13, no. 12, p. 55, 2020, doi: [10.3390/en13123055](https://doi.org/10.3390/en13123055).
- [14] C. Rossi, D. Pontara, C. Falcomer, M. Bertoldi, and R. Mandrioli, "A Hybrid–Electric Driveline for Agricultural Tractors Based on an e-CVT Power-Split Transmission," *Energies*, vol. 14, no. 21, p. 6912, 2021, doi: [10.3390/en14216912](https://doi.org/10.3390/en14216912).
- [15] D.-D. Tran, M. Vafaeipour, M. El Baghdadi, R. Barrero, J. Van Mierlo, and O. Hegazy, "Thorough state-of-the-art analysis of electric and hybrid vehicle powertrains: Topologies and integrated energy management strategies," *Renew. Sust. Energ. Rev.*, vol. 119, p. 109569, 2020, doi: [10.1016/j.rser.2019.109596](https://doi.org/10.1016/j.rser.2019.109596).
- [16] H.L. Husted, "A comparative study of the production applications of hybrid electric powertrains," *SAE Tech. Paper*, 2003-01-2307, 2003, doi: [10.4271/2003-01-2307](https://doi.org/10.4271/2003-01-2307).
- [17] J.M. Miller, "Hybrid electric vehicle propulsion system architectures of the e-CVT type," *IEEE Trans. Power Electron.*, vol. 21, no. 3, pp. 756–767, 2006, doi: [10.1109/tpel.2006.872372](https://doi.org/10.1109/tpel.2006.872372).
- [18] C. Mansour and D. Clodic, "Dynamic modeling of the electro-mechanical configuration of the Toyota Hybrid System series/parallel power train," *Int. J. Automot. Technol.*, vol. 13, no. 1, pp. 143–166, 2011, doi: [10.1007/s12239-012-0013-8](https://doi.org/10.1007/s12239-012-0013-8).
- [19] H.L. Benford and M.B. Leising, "The lever analogy: A new tool in transmission analysis," *SAE Trans.*, vol. 90, pp. 429–437, 1981, doi: [10.4271/810102](https://doi.org/10.4271/810102).
- [20] J. Liu and H. Peng, "A systematic design approach for two planetary gear split hybrid vehicles," *Veh. Syst. Dyn.*, vol. 48, no. 11, pp. 1395–1412, 2010, doi: [10.1080/00423114.2010.512634](https://doi.org/10.1080/00423114.2010.512634).
- [21] J. Gonzalez and C. Sueur, "Unknown input observer with stability: A structural analysis approach in bond graph," *Eur. J. Control.*, vol. 41, pp. 25–43, 2018, doi: [10.1016/j.ejcon.2018.01.006](https://doi.org/10.1016/j.ejcon.2018.01.006).
- [22] B. Li, D. Sun, M. Hu, X. Zhou, J. Liu, and D. Wang, "Coordinated control of gear shifting process with multiple clutches for power-shift transmission," *Mech. Mach. Theory*, vol. 140, pp. 274–291, 2019, doi: [10.1016/j.mechmachtheory.2019.06.009](https://doi.org/10.1016/j.mechmachtheory.2019.06.009).
- [23] B. Li, D. Sun, M. Hu, X. Zhou, D. Wang, Y. Xia, and Y. You, "Automatic gear-shifting strategy for fuel saving by tractors based on real-time identification of draught force characteristics," *Biosyst. Eng.*, vol. 193, pp. 46–61, 2020, doi: [10.1016/j.biosystemseng.2020.02.008](https://doi.org/10.1016/j.biosystemseng.2020.02.008).